



# Experimental investigation of nucleate pool boiling characteristics of high concentrated alumina/water nanofluids

Jagdeep M. Kshirsagar<sup>1</sup> · Ramakant Shrivastava<sup>1</sup>

Received: 4 March 2017 / Accepted: 7 December 2017 / Published online: 12 January 2018  
© Springer-Verlag GmbH Germany, part of Springer Nature 2018

## Abstract

In Present study, the critical heat flux (CHF) and boiling heat transfer coefficient of alumina nanoparticles with the base fluid as deionised water is measured. The selected concentrations of nanofluids for the experimentation are from 0.3, 0.6, 0.9, 1.2 and 1.5 wt%. The main objective to select higher concentration is that to study the surface morphology of heater surface at higher concentrations and its effect on critical heat flux and heat transfer coefficient. It is observed that the critical heat flux enhancement rate decreases as concentration increases and surface roughness of heater surface decreases after 1.2 wt% concentration of nanofluids.

## Nomenclature

### Abbreviations

A	Area of heater surface, [m <sup>2</sup> ]
CHF	Critical Heat Flux
D	Diameter of heater, [m]
$h_{fg}$	Latent heat of vaporization, [kJ/kg]
I	Current [Ampere]
L	Length of heater, [m]
$\rho_l$	Density of liquid [kg/m <sup>3</sup> ]
$\rho_v$	Density of vapour
$q''_{CHF}$	Critical heat flux, [MW/m <sup>2</sup> ]
$R_a$	Average roughness [μm]
SEM	Scanning electron microscopy
$T_s$	Temperature of heater surface, [°C]
$T_{sat}$	Saturation temperature, [°C]
V	Voltage [Volts]

### Greek symbols

$\Delta$	Difference
$\sigma$	Surface tension, [N/m]
$\lambda$	X- ray wavelength of vapour jets, [m]
$\theta$	Peak, [radian]
$\beta$	Full width half maxima of the peak, [radian]
$\nu$	Frequency, [Hz]
$\rho$	Density, [kg/m <sup>3</sup> ]

### Subscripts

C	Critical
fg	Vaporization

HF	Heat flux
l	Liquid
sat	Saturation
v	Vapour

## 1 Introduction

Nanofluids are a new heat transfer fluids, engineered by dispersing and stably suspending nanoparticles in conventional heat transfer fluids. The base fluids include deionized water, ethylene, oil, bio fluids, Refrigerants and polymer solutions. Nanofluids originally involved great interest because of their abnormally enhanced thermal conductivity. Increasing interests have been paid to, as they are potential fluids for heat transfer enhancement. A concert shown by nanofluids makes them a candidate for improved heat transfer media. The base fluids used for study of heat transfer are deionised water (DW), ethylene glycol (EG), glycerol, silicone oil, and the dual mixture of DW and EG. Various nanoparticles involving Al<sub>2</sub>O<sub>3</sub> nanoparticles with different sizes, SiC nanoparticles with different shapes MgO, ZnO, SiO<sub>2</sub> Fe<sub>3</sub>O<sub>4</sub> and TiO<sub>2</sub> nanoparticles and carbon nanotubes with different pre-treatment are used as additives.

Heat transfer is a significant matter in various engineering and commercial applications. The heat transfer in the nucleate boiling regime, the latent heat of vaporization during the change from liquid to gas phase can be oppressed and is the most effective way of cooling thermal systems functioning at high temperatures [1]. However, the boiling heat transfer is constrained by the critical heat flux (CHF). It is uppermost

Ramakant Shrivastava is the first authors

✉ Ramakant Shrivastava  
ramakant.shrivastava@gmail.com

Jagdeep M. Kshirsagar  
jmk\_swayam@rediffmail.com

<sup>1</sup> Department of Mechanical Engineering, Government Engineering College, Aurangabad, India

heat flux where boiling heat transfer sustains its high cooling performance. When the surface reaches CHF, it becomes coated with a vapour film which isolates the heating surface and the fluid thus the heat transfer decreases significantly [1–4]. In these conditions, the wall temperature rises quickly, and when it exceeds the limits of its constituent materials, system failure occurs. For this reason, every system incorporates a safety margin by running at a heat flux lower than CHF, but this approach reduces system efficiency [1]. This compromise between safety and efficiency is a severe problem in the engineering. For this reason, massive work has been carried out to comprehend heat transfer mechanisms in nucleate boiling and CHF situation and to increase the critical heat flux.

Pirotto et al. present a very well review of the parametric effect of boiling surface and prediction methods. They show that it is compound problems involving many inter linked parameters affect heat transfer performances. Their analysis of the literature shows that some results seem incongruous. For example, some researchers conclude that for many practical applications the effect of solid/liquid/vapour interaction on the heat transfer coefficient in nucleate boiling conditions can be ignored (except for the cryogenic fluid), whereas others conclude that these effects are important [5, 6]. Some studies have firm on evaluating the effect of surface characteristics on heat transfer performance. These parameters are typically the contact angle, thermo physical properties, thickness, orientation in space, roughness (surface finish), and microstructure (shape, dimensions, pore density for the vapour bubble generating centre) [5, 6]. All these interlinked parameters simultaneously affect heat transfer performance. At the instant, there is not enough information to resolve this complex problem and for this reason, only separate effects are considered [5]. Enhancement in CHF also noted in the literature for all nanofluids with different orientation of heaters and heater surfaces [6].

Micro-structure and wettability are the most important aspects. These parameters are dealt with in the literature, remarkably, Kamatchi R worked on reduced graphene oxide (rGO) is synthesized from graphite powder and various characterization techniques has been used to study the in plane crystallite size, number of layers, presence of functional groups and surface morphology. The rGO flakes dispersed in Millipore water to obtain different weight concentrations of nanofluids, experiment for nucleate pool boiling performed at different weight concentrations and surfaces and obtained results as enhancement in heat transfer coefficient up to 0.001 wt% and deterioration beyond this in smooth surfaces and increases in heat transfer coefficient for SBS and shows maximum enhancement about 60% in comparison with smooth surface at 0.002 wt% [7].

Kong et al. Studied the pool boiling heat transfer performance on a smooth silicon chip surface with agitation was experimentally investigated. The nanofluids (Ag/alcohol) of 0.02% volume concentration and ethyl alcohol with purification over 99.9% were the two contrast working fluids [7].

## 2 Structural and microstructure of Al<sub>2</sub>O<sub>3</sub> nanoparticles

The structural and microstructure properties of the Al<sub>2</sub>O<sub>3</sub> nanoparticles are as follows; Fig. 1 Shows XRD patterns of Al<sub>2</sub>O<sub>3</sub> particles.

### 2.1 Structure analysis Al<sub>2</sub>O<sub>3</sub> of nanoparticles

Figure 1 shows the XRD pattern of Al<sub>2</sub>O<sub>3</sub> nanoparticles. All the peaks in diffraction pattern shows monoclinic structure of Al<sub>2</sub>O<sub>3</sub>, and the peaks The average grain size calculated by using Debye-Scherrer formula as given below is approximately 30 nm where as average size is given 30-50 nm by seller (Table 1).

$$D = 0.9\lambda / \beta \cos\theta \quad (1)$$

Where  $\beta$  is full width at half maxima of the peak in XRD pattern,  $\theta$  is angle of the peak, wavelength of X-rays. Elastic strain is also calculated from XRD results. The strain results suggested that if the particle size is less than 20 nm than they have more strain and greater than 50 nm particles have less strain.

### 2.2 Preparation of nano fluid and characterization

The Al<sub>2</sub>O<sub>3</sub> nanoparticles were procured from Nanoshel LLC USA, having 99% purity with an average size of 30 nm. Magnetic stirring was performed for 6 h just before pool boiling experiments. It is already reported that nanoparticles dispersed without other additives do not change the surface tension of the base fluid.

It is also observed that all Alumina nanoparticles remained in pure Al<sub>2</sub>O<sub>3</sub> state. The SEM photograph of nanopowder is shown in Fig. 2.

#### 2.2.1 Preparation of Al<sub>2</sub>O<sub>3</sub>-water nanofluids by two-step method

In present work, nanofluids are prepared by the two-step method, dispersing dry nanoparticles into the base liquid followed by magnetic stirring. Deionized water is used as the base liquid, and Al<sub>2</sub>O<sub>3</sub> nanoparticles were used without the addition of additives.

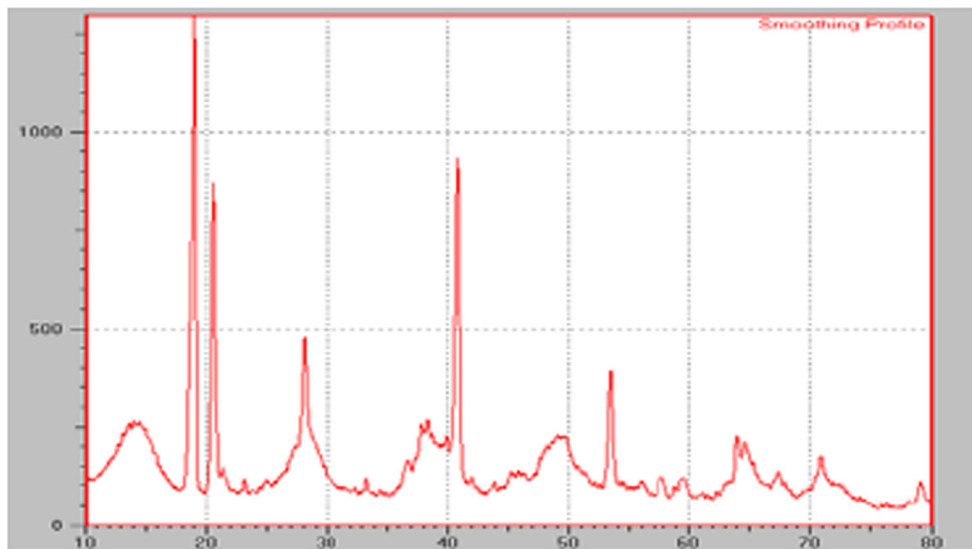


**Fig. 1** XRD pattern of  $\text{Al}_2\text{O}_3$  nanoparticle

The Alumina nanoparticles were dispersed in deionized water for 12 h under high speed mechanical stirrer (Toshiba, India). No surfactant or stabilizer is used during the preparation of nanofluid as they have some influence on forced convective heat transfer coefficient as well as on Overall heat transfer coefficient. After 24 h no sedimentation of nanoparticles were found. Generally, the properties of the nano-fluid depend on the properties of the nano-particles and the surface molecules taking part in the heat transfer procedure depend on the size and shape of the particles themselves, which are also affected by the agglomeration of the particles.

The samples are collected at different weight concentrations as shown in the Fig. 3. The characteristics of nanofluids are governed by not only the kind and size of the nanoparticles but also their dispersion status in the base fluid, it is essential to have the test fluid sample without any agglomeration.

The test fluid sample was collected in a glass vessel and left for 1 to 1.5 h to verify any agglomeration of the particle and subsequent settling in the vessel bottom. It is found that negligible agglomeration in the first 45 min. Considering the duration of the test run which is roughly 4.5 to 5 min, no agglomeration for the first

65 to 70 min was more than enough to get reliable results from the experimentation.

### 3 Experimental set up of pool boiling

Experimental set up was designed and fabricated to carry the experimentation for determination of critical heat flux using deionized water and nanofluids of  $\text{Al}_2\text{O}_3$  materials and weight concentrations. Schematic diagram is shown in the Fig. 4.

It consists of a boiling vessel of capacity 3000 ml capacity of Borosil glass so that the phenomenon of boiling can be visualised. The test section consist of two Bakelite plates as shown in Fig. 5, the top plate and lower plates are fixed with nut and bolt arrangement and has a hole at centre for condenser which is used to cooled the vapour and to maintain the nanofluids constant in the vessel. The copper rods are fixed with nut and bolt arrangement to the lower bakelite plate at a distance about 55 mm from the centre of the opening. The arrangement for thermocouple is made to measure the pool temperature as well as surface temperatures. The test section discussed as below.

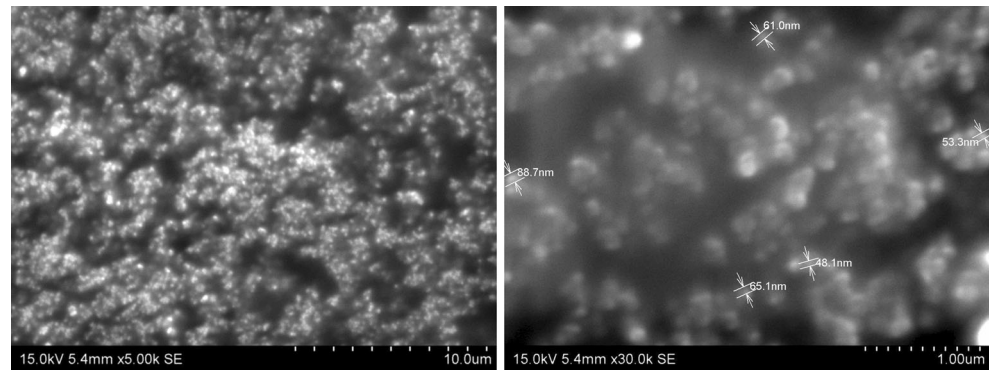
#### 3.1 Test section

Two bakelite sheets are used in test rig as shown in the Fig. 5. Top bakelite cover is used to cover the top side of the glass container so that the vapour will not leave the container. Bakelite has low thermal conductivity to reduce unwanted heat loss. It has a hole at the centre to fix the condenser which is used to condense the vapours escaping from container to maintain constant nanofluids level inside the container. Top bakelite cover also having small holes for thermocouple and

**Table 1** Properties of  $\text{Al}_2\text{O}_3$  nanoparticles

Items	$\text{Al}_2\text{O}_3$
Colour/Content of $\text{Al}_2\text{O}_3$	White/ Alpha-99%
Average particle size	30 nm (30–50 nm)
Morphology	Spherical
Specific Surface Area	130–140 $\text{m}^2/\text{g}$

**Fig. 2** SEM image of  $\text{Al}_2\text{O}_3$  particles at magnifications 10  $\mu\text{m}$  and 1  $\mu\text{m}$



wire to supply current to copper electrodes and to measure temperature as shown in the Fig. 5.

The wire diameter is uniform throughout the length, before experiment the Ni-Cr wire is tested for purity in the laboratory, as per testing report, wire contains 80.06% Nickel, Chromium 19.90 and carbon 0.04%. There is one inner Bakelite plate inserted inside the container to hold four copper electrodes. Bakelite top cover and inner bakelite disk are bolted to each other to hold firmly. To avoid the escape of vapour; silicate paste is pasted on bottom side of top bakelite cover so that the flexible layer will form on bottom side of Top Bakelite cover and after bolting top Bakelite to the base steel frame, the vapour will not escape from side. The thickness of bakelite sheet is 15 mm.

### 3.1.1 Thermocouples

Two thermocouples are used to measure the temperature of surface heater wire. In this investigation K type thermocouples are used, overall insulation is glass braid arrangement. The

temperature range of the thermocouples is from 0  $^{\circ}\text{C}$  to 350  $^{\circ}\text{C}$ , while the insulation is rated up to 482  $^{\circ}\text{C}$ . Before performing experiment each thermocouple is cleaned. Data recorded with *LABVIEW13* data acquisition system.

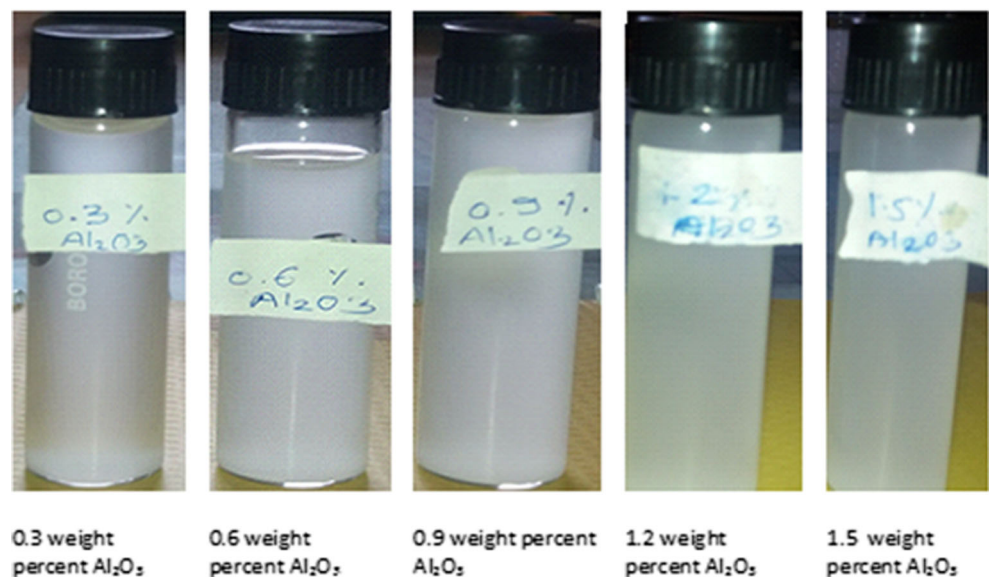
### 3.2 Validation of experimental set up

The Critical heat flux (CHF) condition in nucleate pool boiling that is the critical heat flux can be predicted with reasonable accuracy. The maximum (or critical) heat flux in nucleate pool boiling was determined theoretically by S. S. Kutateladze in Russia in 1948 [8] and N. Zuber in the United States in 1958 using quite different approaches, It is expressed as [9].

$$q'' = C \times h_{fg} [\sigma \times g \times \rho_v^2 (\rho_l - \rho_v)]^{1/4} \text{ W/m}^2 \quad (2)$$

Where  $C$  is constant and value depends on the heater geometry. Critical heat flux is independent of the fluid–heating

**Fig. 3** Samples of  $\text{Al}_2\text{O}_3$  nanofluids at different weight concentrations



0.3 weight percent  $\text{Al}_2\text{O}_3$

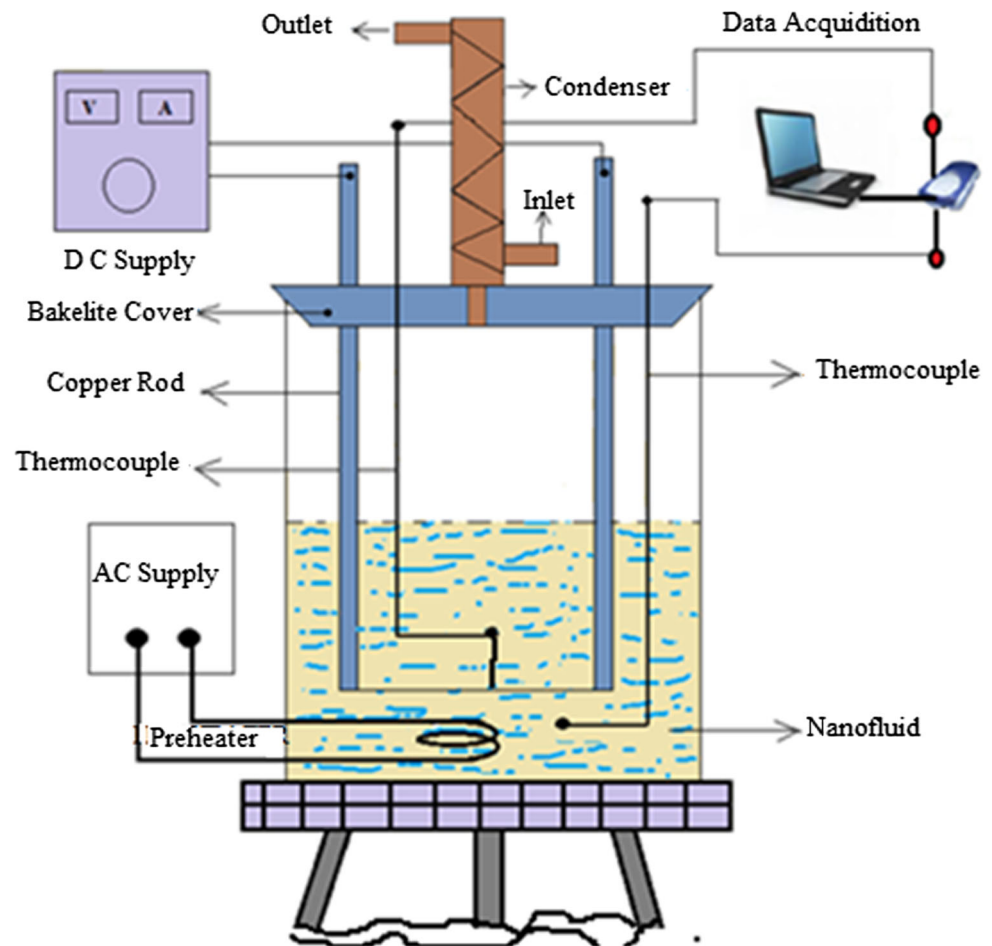
0.6 weight percent  $\text{Al}_2\text{O}_3$

0.9 weight percent  $\text{Al}_2\text{O}_3$

1.2 weight percent  $\text{Al}_2\text{O}_3$

1.5 weight percent  $\text{Al}_2\text{O}_3$

**Fig. 4** Schematic diagram of pool boiling Apparatus for nanofluid



surface combination, as well as the viscosity, thermal conductivity and the specific heat of the liquid.

Exhaustive experimental studies by Lienhard and his co-workers indicated that the value of  $C$  is about 0.149 for large flat plate heater [10].

Zuber's analysis yielded for horizontal cylinder,

$$C = \pi/24 \quad C = 0.1309 \sim 0.131$$

Hence The Zuber's equation (28) for the peak flux (in  $\text{W}/\text{m}^2$ ) in saturated pool boiling is

$$q_z'' = 0.131 \times h_{fg} [\sigma \times g \times \rho_v^2 (\rho_l - \rho_v)]^{1/4} \quad \text{W}/\text{m}^2 \quad (3)$$

Value of  $C$  is taken as 0.131 for cylindrical surfaces Ni-Cr Wire experimentations. Zuber's correlation predicts critical heat flux in nucleate pool boiling using cylindrical heater surfaces with acceptable accuracy it is shown in Fig. 6 as theoretical values of CHF. It is widely acceptable correlation as per open literature [8, 9]. Present study uses Zuber's correlations to predict critical

heat flux within  $\pm 5.18\%$  of band. For deionized water at saturated temperature (i.e. at  $100^\circ\text{C}$  temperature and atmospheric pressure. The Fig. 6 shows the comparative analysis between theoretical and experimental values of CHF of deionized water.

### 3.3 Uncertainty analysis

In the current investigation, the heat fluxes and the heat transfer coefficient for experimental data were reported. The uncertainty of those calculated values are presented.

$$\frac{\Delta q}{q} = \sqrt{\left(\frac{\Delta V}{V}\right)^2 + \left(\frac{\Delta I}{I}\right)^2 + \left(\frac{\Delta d}{d}\right)^2 + \left(\frac{\Delta L}{L}\right)^2}$$

$$\frac{\Delta q}{q} = \sqrt{(1.65)^2 + (2.689)^2 + (0.31)^2 + (1.81)^2}$$

$$\frac{\Delta q}{q} = 6.45\%$$

Using the formulae above, the uncertainty of each data point was calculated.

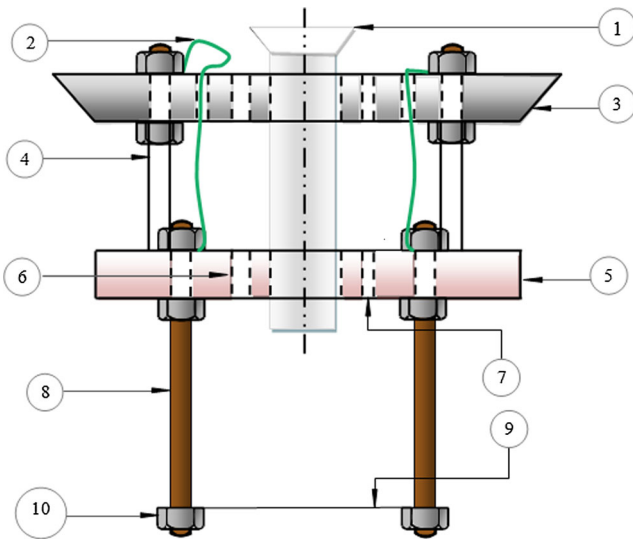


Fig. 5 Schematic view of bakelite covers and test section

## 4 Result and discussions

The pool boiling experiments are performed for different weight concentrations  $Al_2O_3$  nanofluids.

### 4.1 Pool boiling experiments with $Al_2O_3$ nanofluids

Pool boiling behaviour of  $Al_2O_3$  nanofluid at different weight concentrations is observed at atmospheric pressure. The experimental result shows that the percentage of enhancement in critical heat flux is decreased as the weight concentration of nanofluids is increased. The characterization heater surface is after pool boiling experiment and before experiment is carried out by scanning electron microscopy (SEM) image and measuring surface roughness which is discussed separately.

Sr.No.	Name of Component	Sr.No.	Name of Component
1	Opening for Condenser	2	Cable Connected to Copper Rod
3	Upper Bakelite Plate	4	Copper rods to fix Bakelite plates
5	Lower Bakelite Plate	6	Hole for RTD/Thermometer/ K-Thermocouple
7	Hole for K-thermocouple	8	Copper Rods
9	Ni-Cr Wire	10	Nut and Bolt Arrangement to fix Ni-Cr wire

Fig. 6 Comparative values of CHF theoretical and experimental

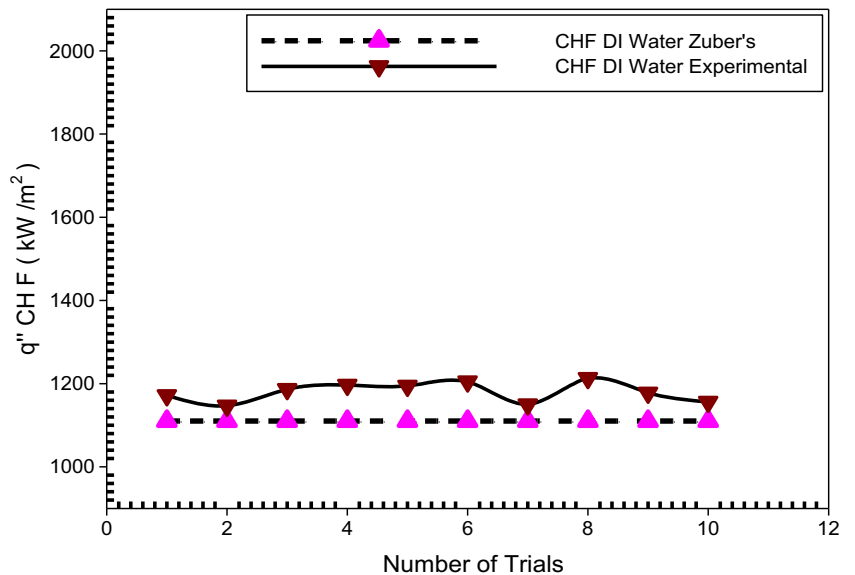
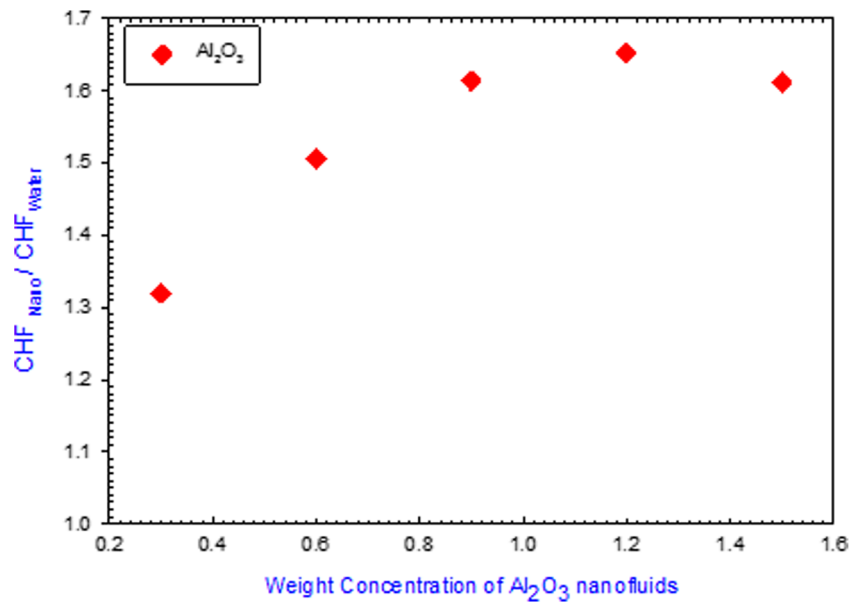


**Fig. 7** CHF of water- $\text{Al}_2\text{O}_3$  nanofluids on Ni-Cr Wire



#### 4.1.1 Effect of nanofluid concentrations

Experiments are performed to determine the heat flux of  $\text{Al}_2\text{O}_3$ -water nanofluid, deionised water is used as the base fluids and different weight concentrations 0.3, 0.6, 0.9, 1.2 and 1.5 are prepared for the experimentation. As shown in the Fig. 7 different weight concentrations of nanofluids shows enhancement in critical heat flux, at 0.3 wt% of nanofluids the boiling heat transfer increased by 43.1%.

The measured critical heat flux CHF values of  $\text{Al}_2\text{O}_3$  nanofluid at different weight concentration, significant critical heat flux enhancement is observed for all nanofluids up to 87% in  $\text{Al}_2\text{O}_3$  as compare to deionized

water. The maximum enhancement is observed in 1.2 wt% of concentrations of alumina nanofluids is followed by 0.9 wt% of alumina nanofluid, 0.9 and 1.2 wt% of nanofluids the rate of enhancement is less as compare to 0.6 to 1.2 wt%.

As shown in the Fig. 8 different weight concentrations of nanofluids shown enhancement in CHF, at 0.3 wt% of nanofluid boiling heat transfer increased by 45.11% when compare to that of deionized water by further adding  $\text{Al}_2\text{O}_3$  nanoparticles enhancement in CHF takes place, the curve slowly shift towards right and also rate of enhancement is also increases but percent rate of enhancement with increases in percent of concentration decreases.

**Fig. 8** Variation in CHF at different weight concentration  $\text{Al}_2\text{O}_3$  nanofluids

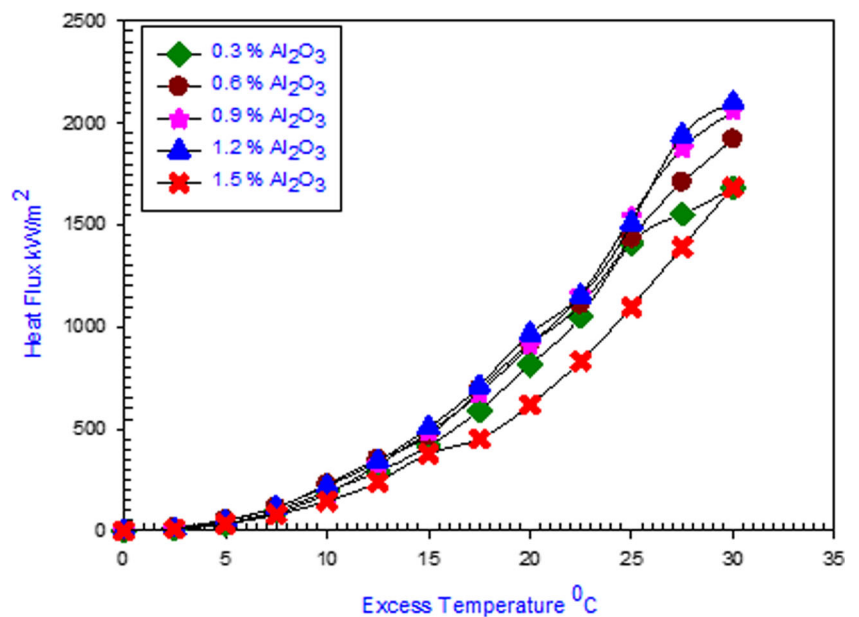
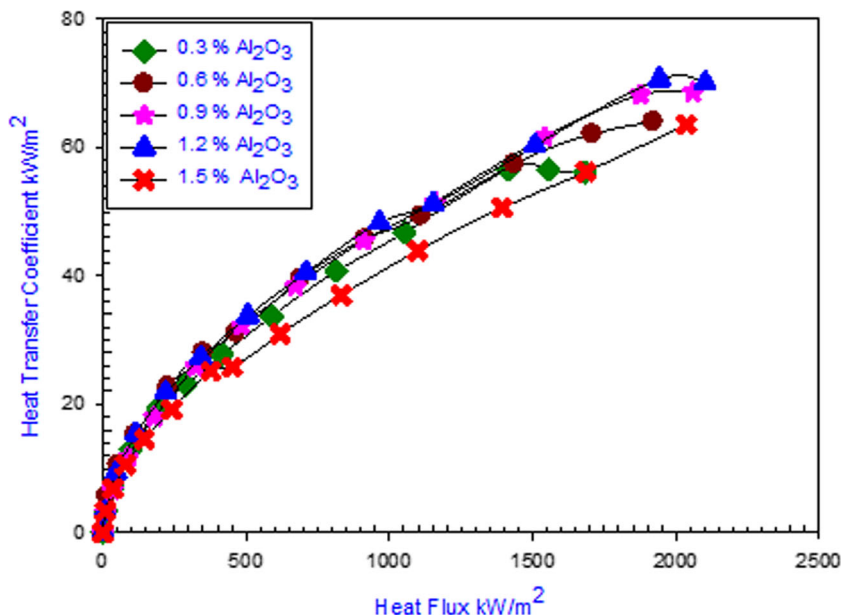


**Fig. 9** Heat transfer coefficient vs heat flux for different wt. con. of Al<sub>2</sub>O<sub>3</sub> nanofluids



The nanofluid has higher critical heat flux when compare to water. Surface roughness measurement of the test wire indicated the accumulation of nanoparticles. This can be attributed to the porous layer formed due to boiling.

As shown in the Fig. 9, heat transfer coefficient of Al<sub>2</sub>O<sub>3</sub> nanofluids at higher concentrations of nanofluids decreases at the same heat flux, the heat transfer coefficient is lower at higher concentrations at 1.2 wt% of alumina it is higher at the same heat flux, at the higher heat flux the effect of concentration is outstanding. It is observed in the Fig. 9 that for the particular concentration, at 1.2 weight concentration in the present study heat flux is highest for the range tested from 0.3 to 1.5 wt% of alumina nanofluid.

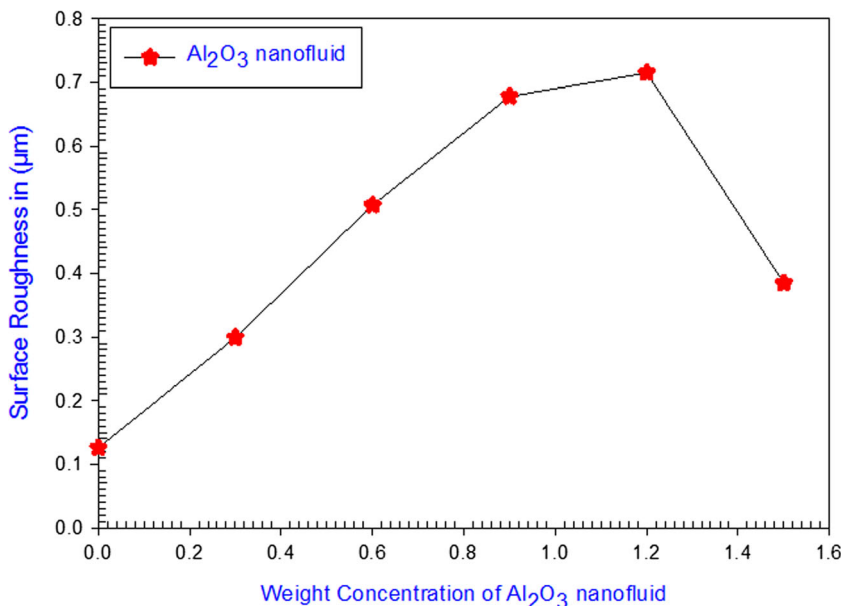
Induced precipitation of nanoparticles which was confirmed by surface testing Fig. 10 shows the variation of surface roughness with different weight concentration of alumina nanofluid.

The presence of a porous layer on the surface plays major role on boiling heat transfer through changes in roughness and wettability. The detailed study of SEM image shows deposition of nanoparticles on the wire surface.

Figure 11 shows SEM image of the bare heater surface and the heater surface after reaching the CHF at different weight. It is observed that deposition is more pronounced on the heater surface with higher weight concentrations.

However in this study peak CHF is at 1.2 where it is observed that surface roughness is higher with other wt. concentrations of Al<sub>2</sub>O<sub>3</sub> nanofluids. Pool boiling

**Fig. 10** Variation in surface roughness with different wt con Of Al<sub>2</sub>O<sub>3</sub> nanofluids





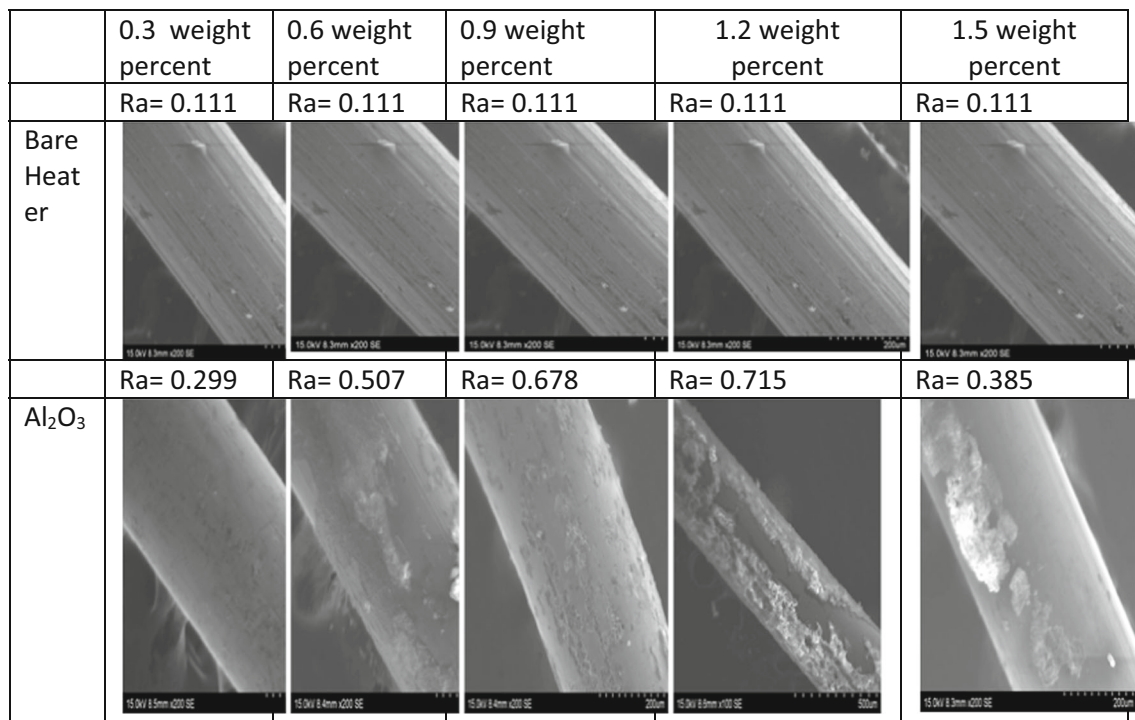


**Fig. 11** SEM Images of heater surface exposed to pool boiling of Al<sub>2</sub>O<sub>3</sub> nanofluid with different weight concentrations

characteristics in Al<sub>2</sub>O<sub>3</sub> nanofluids were investigated with different weight concentrations ranging from 0.3wt.percent to 1.5 wt. percent and effect of nanoparticles in pool boiling CHF of Al<sub>2</sub>O<sub>3</sub> nanofluids for each concentration studied experimentally, during the experimentation the pool boiling CHF of Al<sub>2</sub>O<sub>3</sub> nanofluids on bare heater of Ni-Cr wire was enhanced by 87% compared that of deionized water.

This study clear showed that CHF enhanced of nanofluids was due to nanoparticles surface coating formed on the heater surface during pool boiling surface roughness and measurement and from SEM images of heater surface substantiated this formation of porous layer with micro cavities and deposition of nanoparticles resulted in enhancement of CHF.

## 5 Data interpretation

### 5.1 Effect of nanoparticles on nucleate boiling

The most amazing feature of nucleate boiling in the present experiments was the reduction of the heat transfer coefficient, as revealed by the boiling curve shift to the right. It is interesting to note that the heat transfer deterioration in the nucleate boiling regime was also observed by R. Kamatchi et al. [11] and Bang and Chang [12]. On the other hand, heat transfer enhancement was reported by Dinh et al. [13] and Wen and Ding [14], while You et al. [15] and Vassallo et al. [16]

reported no change of heat transfer in the nucleate boiling regime. Wen and Ding [14] proposed that these conflicting trends could be due to poorly characterized/reported factors such as initial surface roughness, presence of surfactants, agglomeration of particles, surface contamination, etc. A way to capture some of these effects is to consider Wang and Dhir's [17] expression for the nucleation site density:

$$n'' \propto N_c (1 - \cos\theta) ((T_w - T_{sat})^6 \quad (4)$$

Where  $N_c$  is the number of micro cavities per unit surface area and  $T_w - T_{sat}$  is the wall superheat. According to Eq. (4) a decrease of the contact angle would tend to decrease the active nucleation site density and thus the heat transfer coefficient. However, nanoparticles deposition also alters the surface roughness and number of micro cavities present on the surface. In our boiling experiments with stainless steel wire heaters submerged in nanofluids containing metal oxide nanoparticles the number of micro cavities and the surface roughness are typically increased Figs. 10 and 11, which is in agreement with the findings in reference [12]. However, other researchers also reported a decrease in surface roughness upon nanofluid boiling [18]. This clear variation could be due to difference in the size of nanoparticles, initial morphology of the substrate surface, particle deposition rate and duration of the experiment. Deposition of small particles on surfaces with large number of cavities could lead to filling the cavities, thus it will leads to reduce surface roughness of heater surface;

otherwise, deposition of large particles on an initially smooth surface will lead to higher surface roughness. However, lacking direct measurement of the nucleation site density, the link between boiling curve shift and nanoparticles layer cannot be decisively elucidated.

### 5.2 Effect of nanoparticles on CHF

The literature is generally lacking in explaining the CHF enhancement mechanism in nanofluids. Although several decades of passionate study a consensus explanation of the physical mechanism causing CHF is yet to be found even for the simpler case of a pure substance. Hypotheses have been formulated, most of which normally into one of four categories:

Hydrodynamic instability theory [9, 19], macro layer dry out theory [20–22], hot/dry spot theory [23], and bubble interaction theory [8, 24]. Of these four theories, the last three support surface wettability in relation to CHF enhancement. A thorough review of these theories is presented in reference [25]. To illustrate the effect of surface wettability on CHF, a review of the hot/dry spot theory is given below. If the heat flux is high, hot/dry spots develop within the bases of the bubbles growing at certain nucleation sites. The hot/dry spots can be reversible or irreversible. They are reversible if rewetting occurs upon bubble departure. They are irreversible if rewetting does not occur, which causes a runaway excursion of the surface temperature and eventually burnout [26]. In principle the presence of the nanoparticle layer on the surface can help delay CHF in two ways. Its increased wettability promotes rewetting upon bubble departure.

The model proposed by Theofanous and Dinh [13] considered the micro hydrodynamics of the solid-liquid-vapour line at the boundary of a hot/dry spot. They imagine that CHF

occurs when the evaporation recoil force, which drives the liquid meniscus to recede, becomes larger than the surface tension force, which drives the meniscus to advance and rewet the hot/dry spot. On this basis, they derived the following expression for the CHF:

$$q_{cr}'' = k^{-1/2} \rho_g h_{fg} \left[ \left\{ \sigma (\rho_f - \rho_g) g \right| \rho_g^2 \right\}^{1/4} \tag{5}$$

Equation (4) and the traditional Kutateladze-Zuber’s formula [8] are essentially the same, except for the parameter  $\kappa$ , which is the coefficient of proportionality between the radius of curvature of the liquid meniscus less than the capillary length:

$$\kappa \sim \kappa \sqrt{\sigma/g} (\rho_f - \rho_g) \tag{6}$$

Theofanous and Dinh state that  $\kappa$  is a surface dependent parameter that for a well-wetting surface is smaller than for a poorly-wetting surface.

### 5.3 Resistance of heater surface

In the present work pool boiling performance of  $Al_2O_3$  nanofluids at different weight concentration of nanofluids is studied at atmospheric pressure. The experimental result indicated enrichment in boiling heat transfer with  $Al_2O_3$  nanofluid when compared with deionized water. The characterization of heater surface is carried out quantitatively and qualitatively by taking the image of Scanning Electron Microscopy [SEM image] and measuring surface roughness respectively which are discussed in detail in Figs. 10 and 11.

The heat flux (CHF) is determine experimentally by using Eq. 7

**Fig. 12** Experimental and predicted values of heat flux at different wt. concentration of  $Al_2O_3$  nanofluid

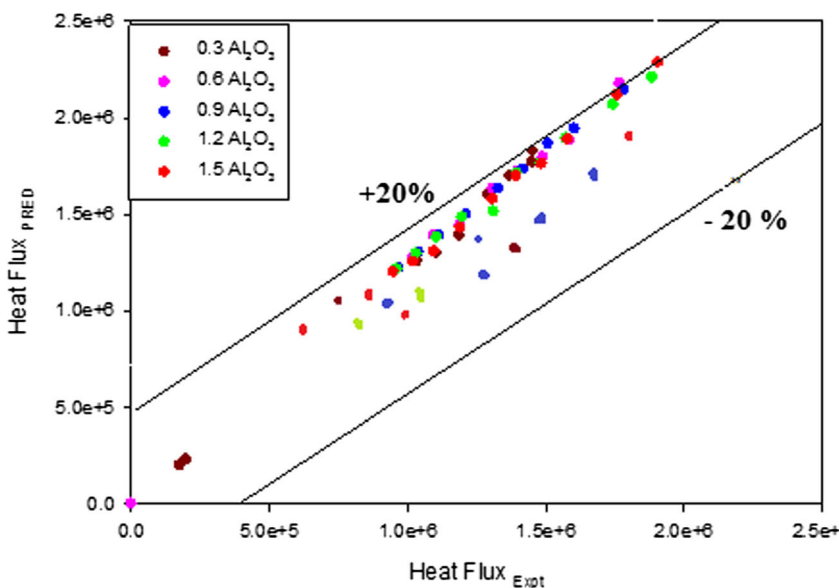
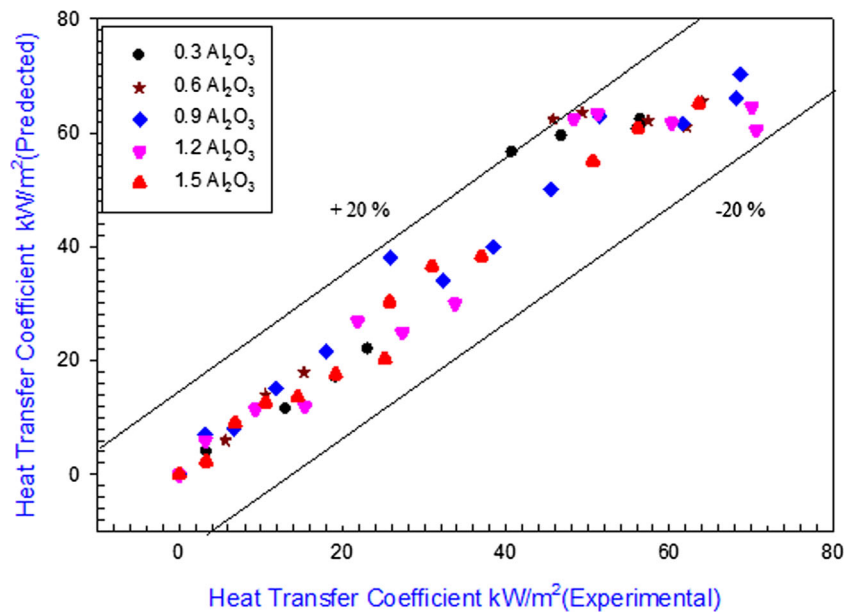


**Fig. 13** Experimental and predicted values of heat transfer coefficient  $\text{Al}_2\text{O}_3$  nanofluids



$$q'' = \frac{V \times I}{\pi \times d \times L} \quad (7)$$

$V$  is voltage in  $\Omega$ ,  $I$  is current in Amp,  $d$  is the diameter of Ni-Cr wire and  $L$  is the length of wire in m and  $q''$  is heat flux  $\text{W}/\text{m}^2$ .

P.Vassallo et al. also measured the system resistance through the power supply, Meters and by connecting lead wire together and measuring the Voltage at low current generally less than 1A, this resistance then subtracted from the resistance measurement obtained with Ni-Cr wire connected to the lead wires. The system resistance was between 0.8 to 0.11  $\Omega$  will be depends on the length of wire [16]

$$R_{\text{wire}} = \frac{V}{I} - R_{\text{system}} \quad (8)$$

Where  $R_{\text{wire}}$  = Ni-Cr wire resistance,  $V$  = measured voltage,  $I$  = measured current and  $R_{\text{system}}$  is system resistance excluding Ni-Cr wire, the system was operated in the range of 1 A to ~10 A for several times.

The boiling curve data were then taken by slowly increasing current and recording voltage and current readings the boiling was initiated at some spots when the current is  $>3$  Amp if the wire was taken to failure  $>12$  Amp the wire will be suddenly break or become red and get break when current was increased. The boiling curves were generated by deriving the wire temperature from known temperature resistance relationship and calculate the heat flux from measured voltage and current [16]. The heat flux was predicted from the Eq. 9.

$$q'' = \frac{I^2 R_{\text{wire}}}{2\pi r l} \quad (9)$$

The result of the present work compared with the Eq. 9 and predicted and experimental.

Values of CHF and heat transfer coefficient are calculated which are shown in the Figs. 12 and 13 respectively, it shows well agreement within the range of  $\pm 20\%$  error band.

## 6 Conclusion

In this study, pool boiling CHF behaviours on electrically heated Ni-Cr wire with nano-porous deposits were investigated at saturated temperature under atmospheric pressure. Various deposit structures were obtained by varying the increasing rate and maximum value of heat flux during the pre-boiling in different weight concentration of water-Alumina nanofluid. Surface properties of the deposit wires were characterized to identify the major surface parameters associated with the significant CHF increases on a heater with nanoparticles deposits. It was found that heat capacity of heater surface in the present study changes due to the nanoparticles deposit so that it is not a major parameter in interpreting the increased CHF. Pool boiling characteristics in Alumina nanofluid were investigated with five weight concentrations 0.3, 0.6, 0.9, 1.2 and 1.5 wt% of Alumina with deionised water. The enhancement in CHF for every concentration is studied; the maximum enhancement of 87% CHF takes place at 1.5 wt% of Alumina and for 0.3 wt% 43.1%.

During experimentation it is observed that roughness on heater surface increases up to 1.2 wt. percent after that it suddenly decreases, even CHF increases slowly from 1.2. to 1.5 wt. percent, rate of enhancement in CHF decreases from 1.2 to 1.5 wt. Percent of Alumina nanofluid. CHF enhancement is directly related with surface microstructure and enhanced topography resulting from the deposition of nanoparticles SEM image of the heater surface shows porous layer build up due to boiling induced precipitation of nanofluid. Decrease in surface roughness can be attributed to nanoparticles filling the micro cavities formed over the heater surface.

## References

- Kim S, Kim HD, Kim H, Ahn HS, Jo H, Kim J, Kim MH (2010) Effects of nano-fluid and surfaces with nano structure on the increase of CHF. *Exp Thermal Fluid Sci* 34:487–495
- Özsisik MN (1985) *Heat transfer: a basic approach*. McGraw-Hill International Editions, New York
- Collier JG, Thome JR (2001) *Convective boiling and convection*, third edn. Oxford Science Publication, Oxford
- Kshirsagar JM, Shrivastava R (2015) Review of the influence of nanoparticles on thermal conductivity, nucleate pool boiling and critical heat flux. *Heat Mass Transf* 51:381–398. <https://doi.org/10.1007/s00231-014-1412-3>
- Pirol IL, Rohsenow W, Doerffer SS (2004) Nucleate pool-boiling heat transfer. I: review of parametric affects of boiling surface. *Int J Heat Mass Transf* 47:5033–5044
- Pirol IL, Rohsenow W, Doerffer SS (2004) Nucleate pool-boiling heat transfer. II: review assessment of prediction methods. *Int J Heat Mass Transf* 47:5045–5057
- Kong et al (2016) Boiling heat transfer enhancement of nanofluids on a smooth surface with agitation. *Heat Mass Transf* 52(12):2769–2780
- Kutateladze SS (1952) *Heat transfer in condensation and boiling*. U.S. AEC Report AEC-tr—3770. Moscow, Russia: State Science and Technology Publications of Literature on Machinery
- Zuber N (1959) *Hydrodynamic aspects of boiling*. U.S. Atomic Energy Commission Rept., AECU - 4439. Tech. Inf. Serv., Oak Ridge
- Bakhr N, Lienhard JH (1972) Boiling from small cylinders. *Int J Heat Mass Transf* 15(11):2011–2025
- Hegde RN, Rao SS, Reddy RP (2012) Experimental studies on CHF enhancement in pool boiling with CuO-water nanofluid. *Heat Mass Transf* 48:1031–1041
- Bang C, Chang SH (2005) Boiling heat transfer performance and phenomena of Al<sub>2</sub>O<sub>3</sub>-water nano-fluids from a plain surface in a pool. *Int J Heat Mass Transf* 48:2407–2419
- Dinh TN, Thu JP, Theofanous TG (2004) Burnout in high heat flux boiling: the hydrodynamic and physicochemical factors. 42nd AIAA Aerospace Sciences Meeting and Exhibit, Nevada
- Wen D, Ding Y (2005) Experimental investigation into the pool boiling heat transfer of aqueous based  $\gamma$ -alumina nanofluids. *J Nanopart Res* 7:265–274
- You SM, Kim J, Kim KH (2003) Effect of nanoparticles on critical heat flux of water in pool boiling heat transfer. *Appl Phys Lett* 83(16):3374–3376
- Vassallo P, Kumar R, D'Amico S (2004) Pool boiling heat transfer experiments in silica-water Nano-fluids. *Int J Heat Mass Transf* 47:407–411
- Wang CH, Dhir VK (1993) Effect of surface wettability on active nucleation site density during pool boiling of water on a vertical surface. *J Heat Transf* 115:659–669
- Kamchi R et al (2016) Experimental investigation and mechanism of critical heat flux enhancement in pool boiling heat transfer with nanofluids. *Heat Mass Transf* 52(11):2357–2366
- Haramura Y, Katto Y (1983) A new hydrodynamic model of CHF applicable widely to both pool and forced convection boiling on submerged bodies in saturated liquids. *Int J Heat Mass Transf* 26:389–399
- Sadasivan P, Chappidi PR, Unal C, Nelson RA (1992) Possible mechanisms of macrolayer formation. *Pool and External Flow Boiling* (ASME 1992). ASME, New York, p 135
- Katto Y, Yokoya S (1968) Principal mechanism of boiling crisis in pool boiling. *Int J Heat Mass Transf* 11:993–1002
- Theofanus TG et al (2002) The boiling crisis phenomenon. Part II: dry out dynamics and burnout. *Exp Thermal Fluid Sci* 26:793–810
- Rosenhow W, Griffith P (1956) Correlation of maximum heat flux data for boiling of saturated liquids. *Chem Eng Prog Symp Ser* 52(18):47–49
- Kolev N (2002) How accurately can we predict nucleate boiling? In: *Multiphase Flow Dynamics vol 2*. Springer, Berlin
- Kim S, Bang IC, Buongiorno J, Hu LW (2007) Surface wettability change during pool boiling of nanofluids and its effect on critical heat flux. *Int J Heat Mass Transf* 50(2007):4105–4116
- Kamachi R (2017) Experimental investigations on nucleate boiling heat transfer of aqua based reduced graphene oxide nanofluids. *Heat Mass Transf*. <https://doi.org/10.1007/s00231-017-2135-z>